Nano-Structures & Nano-Objects 10 (2017) 9–14

Contents lists available at ScienceDirect

Nano-Structures & Nano-Objects

journal homepage: www.elsevier.com/locate/nanoso

Physical properties of self-assembled zinc chlorin nanowires for artificial light-harvesting materials

Ersan Harputlu [a], Kasim Ocakoglu [a,b,*], Fahrettin Yakuphanoglu [c,**], Anna Tarnowska [d], Daniel T. Gryko [d]

[a] Advanced Technology Research & Application Center, Mersin University, Ciftlikkoy Campus, TR333343, Yenişehir, Mersin, Turkey
[b] Department of Energy Systems Engineering, Mersin University, Tarsus Faculty of Technology, 33480 Mersin, Turkey
[c] Nanoscience and Nanotechnology Laboratory, Faculty of Science, Firat University, 23119, Elazıg, Turkey
[d] Warsaw University of Technology, Faculty of Chemistry, Noakowskiego 3, 00-664 Warsaw, Poland

HIGHLIGHTS

- The electrical conductivity properties of supramolecular nanowires were investigated by C-AFM.
- Chlorophyll-derived supramolecular nanowires.
- The electrical conductivity and charge-carrier mobility of zinc chlorin nanowires were found to be 0.93 S/cm and 5.80 × 10^{-2}cm^2/V s, respectively.

GRAPHICAL ABSTRACT

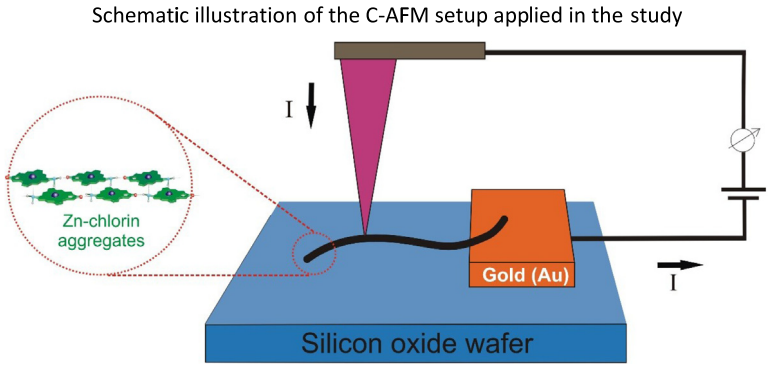

ARTICLE INFO

Article history:
Received 12 October 2016

Keywords:
Artificial photosynthesis
Self-assembled
Zinc chlorins
Chlorophyll
Self-assembly
Aggregation
Conductivity
Nanowires

ABSTRACT

The self-assembled supramolecular structures have recently attracted rising interest in view of their potential application in artificial photosynthesis, supramolecular electronics and many other scientific disciplines. In particular, self-assembled zinc chlorophyll nanowires appear to be highly promising candidates in the field of artificial photosynthesis and organic photovoltaics. In this work, the electrical conductivity properties of chlorosomal rod self-aggregates have been investigated by conductive atomic force microscopy (C-AFM). Two zinc chlorin derivatives bearing different length alkyl chains (ZnChl-C6 and ZnChl-C18) were prepared, and current–voltage characteristics of self-assembled zinc chlorin nanowires were investigated. The electrical conductivity and charge-carrier mobility of zinc chlorin nanowires were found to be 0.93 S/cm and 5.80 × 10^{-2}cm^2/V s, respectively. It is worth noting that these self-assembled zinc chlorin nanowires revealed higher electrical conductivity and the mobility than those of previously published chlorophyll derivative supramolecular nanowires.

1. Introduction

The use of supramolecular interactions for the preparation of photosynthetic light-harvesting (LH) antennas has attracted much attention from the device performance point of view. The

* Corresponding author at: Advanced Technology Research & Application Center, Mersin University, Ciftlikkoy Campus, TR333343, Yenişehir, Mersin, Turkey. Fax: +90 324 361 01 53.
** Corresponding author.
E-mail address: kasim.ocakoglu@mersin.edu.tr (K. Ocakoglu).

http://dx.doi.org/10.1016/j.nanoso.2017.02.002
2352-507X/

construction of highly ordered supramolecular structures and organized on surfaces across multiple length scales represents an important issue within the fast-growing field of light harvesting devices [1–11]. One of the most promising methods for the construction of these supramolecular assemblies relies on the self-organization ability of π-conjugated systems [2,12–18]. Supramolecular nanostructures of self-aggregated zinc chlorin (ZnChl) derivatives have been widely studied due to their intriguing self-organization properties [18–21]. In these studies, surface behaviors of semi-synthetic chlorophyll derivatives that have different molecular structures were investigated in detail by a variety of spectroscopic and microscopic techniques [7,20–23]. It was demonstrated that, aggregation behaviors are largely affected by the molecular structure and the surface properties [7,20–23]. For instance, the presence of hydrophobic hydrocarbon chains at the 17-propionate position (such as farnesyl, cetyl, stearyl, oleyl etc.) of semi-synthetic chlorophyll derivatives not only facilitates the formation of rod/wire aggregates but also allows to obtain more stable aggregates [7,20–23]. From this perspective, it has become easier to obtain desired aggregates different in size and formation. Concerning the charge transport properties, to date, the detailed investigation of such materials was successfully examined only by Würthner and co-workers [8]. In this study, individual nanowires obtained from a semi-synthetic chlorophyll derivative bearing [3′, 5′-bis-(2-{2-[2-(2-methoxyethoxy)ethoxy]ethoxy}ethoxy)] benzyl ester group at the 17 propionate position were investigated by the conductive AFM (C-AFM) method [8]. In order to get a deeper understanding of the charge-carrier transport properties along macroscopic dimensions, a special substrate which consists of a non-conductive silicon oxide surface and a conductive polymer (poly(3,4-ethylenedioxythiophene):poly-(4-styrenesulphonate, PEDOT:PSS)) was used. The conductivity results are promising and comparable in magnitude to those of semiconducting supramolecular oligomers and polymers [8]. However, further detailed investigations are necessary to better understand the supramolecular organization of these nanowires in different environments [24]. Chlorophyll-based dyes are promising candidates for organic photovoltaics as light harvesting materials [25–28]. Indeed, the unique physicochemical properties of chlorophyll pigments make them to be an effective light harvesting material in the concept of artificial photosynthetic systems. The self-organization of biological derivatives on appropriate surfaces is one of the most important parameters in device construction to mimic the analogous natural systems and build suitable artificial solar energy conversion devices. In this regard, the investigation of the electrical conductivity and charge-carrier mobility of the bio-supramolecular nanowires are required for the development of efficient devices.

In the present study, our aim is to investigate the electrical conductivity properties of self-aggregated zinc chlorophyll rod structures organized on surfaces at the nanoscale. To the best of our knowledge, although surface behavior of the compounds used in this study was investigated in detail previously by Shoji et al. [23] due to their proper rod/wire formations, there is only limited information regarding current–voltage characteristics of their rod aggregates in the literature up to now.

2. Experimental

2.1. Materials

All reagents and solvents were purchased from commercial sources. Anhydrous solvents were either distilled from appropriate drying agents or purchased from Merck or Aldrich and degassed prior to use by purging with dry argon and kept in air-tight bottles with molecular sieves. The UV–Vis absorption spectra of

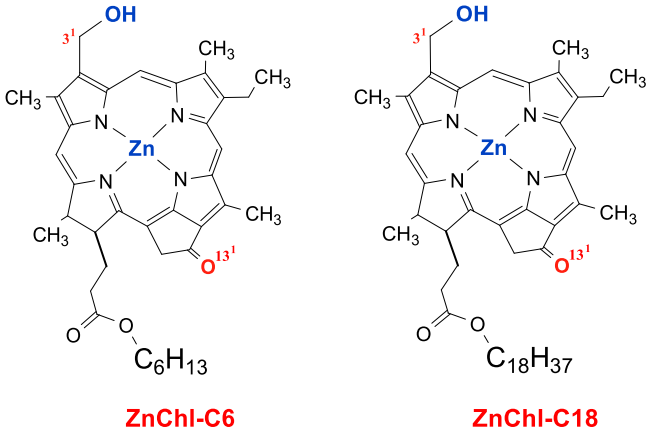

Fig. 1. Chemical structures of zinc chlorin derivatives with different alkyl chains, ZnChl-C6 and ZnChl-C18.

synthesized dyes are recorded in a 1 cm path length quartz cell by using Analytic JENA S 600. The thin conductive gold top layer was prepared by using MiDAS Thermal Vacuum Evaporation System, Pvd PVD/3T. Atomic Force Microscopy (AFM) and Conductive Atomic Force Microscopy (C-AFM) studies were carried out in non-contact and contact modes, respectively using a Park System XE-100 SPM instrument under ambient conditions using a commercial scanning probe microscope. The AFM topographic images were analyzed using Park Systems XEI software. The aggregate solutions of ZnChl-C6 and ZnChl-C18 in THF (Tetrahydrofuran)/n-Hexane (1:99%) were spin-coated (5000 rpm) onto HOPG (Highly oriented pyrolytic graphite) or silicon oxide surfaces and measured under ambient conditions.

2.2. Synthesis of zinc chlorin derivatives

Semi-synthetic chlorophyll derivatives bearing different length of alkyl chains (ZnChl-C6 and ZnChl-C18) were prepared according to the reported procedures [23,26,29] by using chlorophyll-*a* (Chl-*a*) obtained from *Spirulina maxima* algae [30]. Chemical structures of zinc chlorin derivatives are shown in Fig. 1.

3. Results and discussion

3.1. Self-assembly properties of self-aggregated zinc chlorin derivatives in nonpolar organic solvent

The self-assembly properties of semi-synthetic ZnChls in solution were investigated by UV–Vis spectroscopy at the first stage of study. The absorption spectra of the compounds, ZnChl-C6 and ZnChl-C18 in THF/n-hexane (1:99) shown in Fig. 2(a) and (b) reveal a pronounced bathochromic shift of the Q_y band upon self-assembly from 647 nm (monomers) to 741 nm (aggregates) [31–33]. The decrease of the Q_y band of monomer at 647 nm and the increase of the aggregates band at 741 nm was observed upon increasing time. Complete aggregation under such conditions takes up to several hours. At higher concentrations, the 741 nm aggregates form much more rapidly. When close to saturated solutions of ZnChl in THF are diluted with n-hexane, the shift to 741 nm is almost instantaneous on the time scale of our mixing and measuring experiment (within seconds).

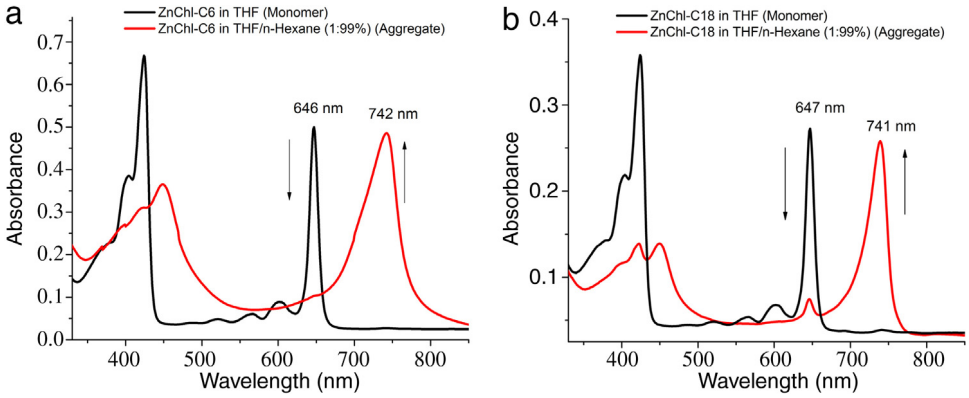

Fig. 2. UV–Vis absorption spectra of the ZnChl derivatives (a) ZnChl-C6, (b) ZnChl-C18 (black-line) monomers in THF; (red-line) solution phase free-standing aggregates in THF/n-Hexane (1:99%). (For interpretation of the references to color in this figure legend, the reader is referred to the web version of this article.)

3.2. Surface morphology properties of self-aggregated zinc chlorin nanowires by AFM studies

The organization and physical properties of well-ordered stacks of ZnChls on HOPG surface were investigated by AFM and C-AFM. The self-aggregation properties of the complexes, ZnChl-C6 and ZnChl-C18, on different surfaces have been investigated previously in detail by Shoji et al. [23]. The supramolecular formation and stability of the zinc chlorins rods which consist of different lengths of an oligomethylene chains at the 17-propionate group have been reported [23]. According to this study, a hydrophobic HOPG substrate was preferred for observing rod/wire self-aggregates by AFM, since the long hydrophobic chains located outside of the rods/wires interacted favorably with a HOPG surface. In this regard, before the investigation the electrical conductivity of molecular nanowires, the formation parameters of the rods were re-examined. A freshly prepared solution of ZnChl in THF/n-hexane (1:99) (100 μM) was deposited by a spin-coating technique on HOPG and allowed to evaporate. Supramolecular nanostructures of semi-synthetic chlorophyll aggregates on a hydrophobic HOPG surface were examined by non-contact mode AFM at room temperature. AFM studies on graphitic surfaces revealed the formation of rod-like structures of different lengths from nanometer to micrometer scales as it was reported before (Figs. 3–4). As it is seen from AFM images, similar structures previously reported by Shoji et al. were successfully obtained before the conductivity studies [23].

3.3. Electrical conductivity properties of the ZnChl-C18 nanowires by Conductive Atomic Force Microscopy (C-AFM)

A commercially available AFM (Park System XE-100 SPM) was used to analyze topographic images and electrical conductivities of the nanowires. The conductivity measurements were performed in contact mode with conductive cantilevers (NSC18/Cr-Au, Mikromasch). A bias voltage in the range 0.5/−0.5 V or 1/−1 V was applied between tip and sample and an external current was used to measure the current during the scanning movement. A silicon wafer with 100 nm oxide layer was used to guarantee a high electrical isolation. Control AFM experiment was performed for the aggregates of ZnChl-C6 and ZnChl-C18 to verify if nanowires are formed on the surface. The thin conductive gold layer was prepared by using MiDAS Thermal Vacuum Evaporation System, Pvd PVD/3T (Vacuum level: 2×10^{-6} Torr, 30 s, thickness: 40 nm). In order to investigate the conductivity properties of the nanowires, a substrate consisted of a non-conductive silicon oxide surface and a gold coated edge which served as a conductive part was prepared (Fig. 5).

Gold layer was especially preferred instead of PEDOT:PSS unlike previous study reported by Sengupta et al. due to difficulties in obtaining a uniform conductive layer [8]. Firstly, a gold contact having 40 nm thickness was prepared on SiO_2 film by a MiDAS thermal evaporator system, PVD/3T. 20 μl of nanowire solution were then deposited on a silicon substrate by spin-coating (Fig. 5). The current–voltage characteristics of the nanowires were investigated by a conducting AFM mode. For this, a nanowire, in which contacts to the conductive gold layer by one end, and the other side lying through the non-conductive silicon oxide surface was chosen randomly, and a voltage was applied between a metal-coated AFM tip and a conductive substrate, as shown in Fig. 5. AFM topography and current images of the ZnChl-C18 nanowires are shown in Fig. 6(a)–(c). Fig. 6(b) shows AFM surface morphology image of the ZnChl-C18 nanowires. As seen in Fig. 6(b), the red regions are conducting while the blue regions are insulator regions. We measured current–voltage (I–V) characteristics of ZnChl-C18 and ZnChl-C6 nanowires to determine electrical conductivity and mobility values. But, we show only I–V characteristics of the ZnChl-C18, as it is seen that I–V characteristics of ZnChl-C18 were much close to that of ZnChl-C6 (Fig. 6(c)). The electrical conductivity of the nanowires is determined from the obtained I–V characteristics using the following relation,

$$\sigma = \frac{I}{V}\frac{d}{A}$$

where σ is the conductivity, I is the current, V is the applied voltage, d is the distance between electrodes and A is the cross sectional area. The electrical conductivity of the ZnChl-C18 nanowires was determined from Fig. 6(c) and was found to be 0.93 S/m. The obtained σ value is higher than that of another type of supramolecular nanowires prepared from chlorophyll derivative dyes [8]. The mobility, μ of the nanowires was calculated by assuming of concentration of the charge carries, 10^{24} charges/m^3. The μ value for the nanowires was found to be 5.80×10^{-2} $cm^2/V\,s$. The obtained mobility is also higher than that of previously published chlorophyll derivative supramolecular nanowires [8]. This suggests that the higher conductivity is due to π-electrons in structure of the ZnChl-C18 nanowires.

AFM topography and current images of the ZnChl-C18 nanowires for various magnifications and bias voltages are shown in Fig. 6. The gold layer in the top part of the image (red color) exhibits a high conductivity compared to the silicon substrate (blue color). The image of a single nanowire which is attached to the gold and shows a current signal is also an obvious confirmation for the electrical conductivity (Figs. 6 and 7). It is necessary to keep constant the loading force of the cantilever during the conductivity measurements. Otherwise, conductivity measurements cannot be performed properly due to the possible deformation on the nanowire caused by the movement of the tip (Fig. 7(b)).

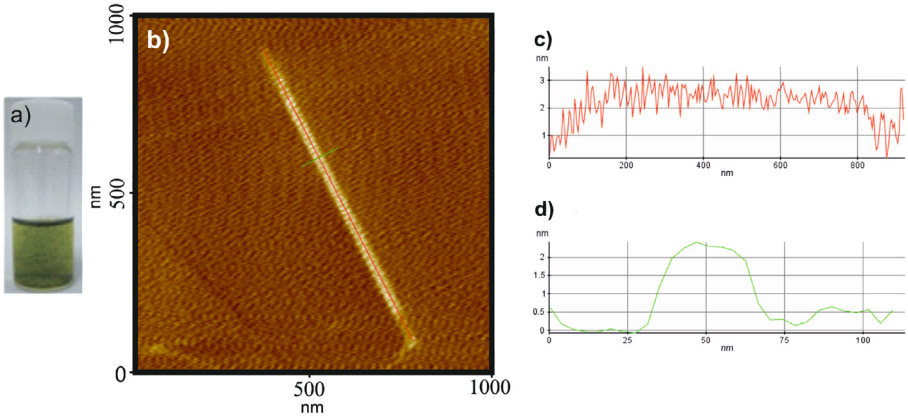

Fig. 3. (a) Photograph of ZnChl-C18 aggregates formed upon dilution of a concentrated THF solution with n-hexane; (b) AFM analysis of self-aggregated ZnChl-C18 on an HOPG substrate; (c) and (d) the length (red line) and height (green line) analysis of the molecular cables. Set point: 3.23 (nN), Z servo gain: 2.69, Scan rate: 0.5 (Hz), Head mode: NC-AFM (Non-contact mode). (For interpretation of the references to color in this figure legend, the reader is referred to the web version of this article.)

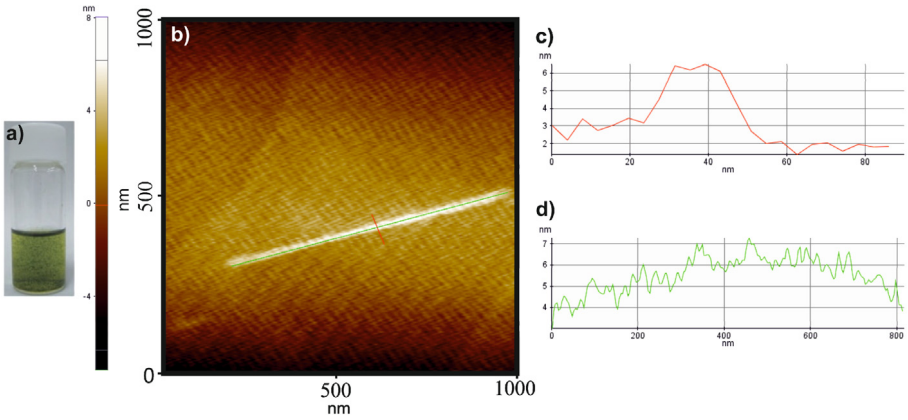

Fig. 4. (a) Photograph of ZnChl-C6 aggregates formed upon dilution of a concentrated THF solution with n-hexane; (b) AFM analysis of self-aggregated ZnChl-C6 on an HOPG substrate; (c) and (d) the height (red line) and length (green line) analysis of the molecular cables. Set point: 2.8 (nN), Z servo gain: 1.58, Scan rate: 0.57 (Hz), Head mode: NC-AFM (Non-contact mode). (For interpretation of the references to color in this figure legend, the reader is referred to the web version of this article.)

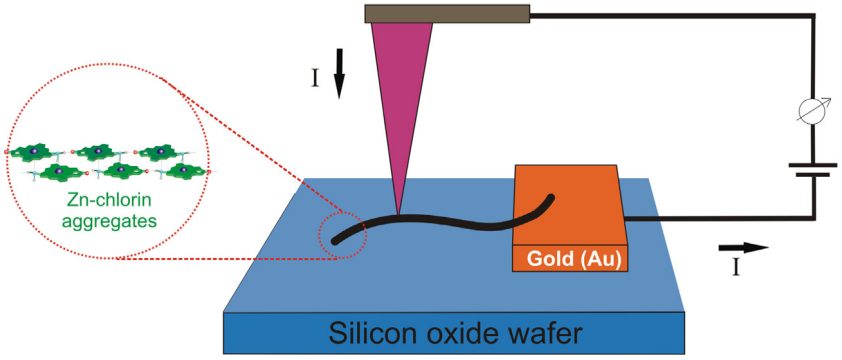

Fig. 5. Schematic illustration of the C-AFM setup applied in the study. In C-AFM mode, a conductive cantilever (claret red) is brought in contact with the nanowire (black). If attached to the gold layer (yellow) upon application of a voltage between tip and sample, a flowing current can be analyzed by an external electronic device. (For interpretation of the references to color in this figure legend, the reader is referred to the web version of this article.)

4. Conclusion

Two zinc chlorin derivatives bearing different length alkyl chains were prepared, and current–voltage characteristics of self-assembled zinc chlorin nanowires were investigated. The electrical conductivity (σ) and charge-carrier mobility (μ) of zinc chlorin nanowires was found to be 0.93 S/cm and 5.80×10^{-2} cm^2/V s, respectively. The self-assembled zinc chlorin nanowires revealed higher electrical conductivity and the mobility than that of another type of supramolecular nanowires prepared from chlorophyll derivative dyes [8]. This result can be explained by the presence of longer oligomethylene chains ($n \geq 6$) which stabilized the nanowires construction by their lipophilic interaction [23]. In particular, the intermolecular interaction between the nanowires which surrounded with hydrophobic oligomethylene chains and hydrophobic HOPG surface are the driving force for the formation of more stable ensembles, which gives rise to very high electrical conductivity and the mobility. These results suggest that, in the application point of view, zinc chlorophyll nanowires appear highly promising in the field of organic photovoltaics and micro-electronics.

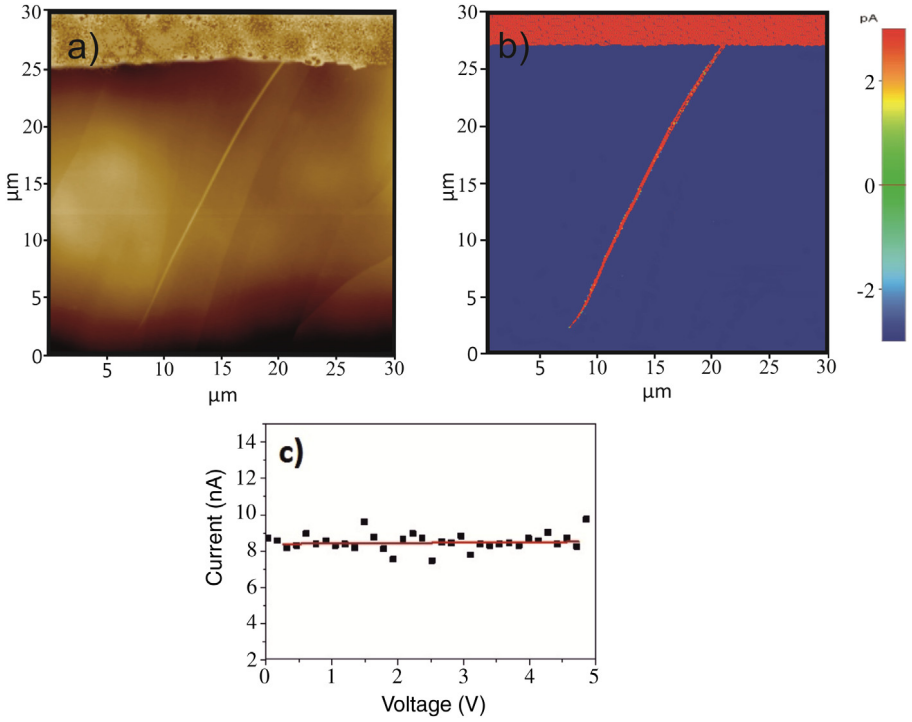

Fig. 6. (a) AFM topography image ($30 \times 30\ \mu m^2$) of single ZnChl-C18 nanowires spin-coated from THF/n-Hexane solution (1:99%) on a silicon oxide surface. Thickness of the gold layer ~40 nm; (b) Corresponding current image measured in the C-AFM mode. Tip bias: 0.5 V, sample bias: −0.5 V, set point: 153.68 (nN), scan rate: 0.66 Hz; (c) I–V characteristics of ZnChl-C18 nanowires. (For interpretation of the references to color in this figure legend, the reader is referred to the web version of this article.)

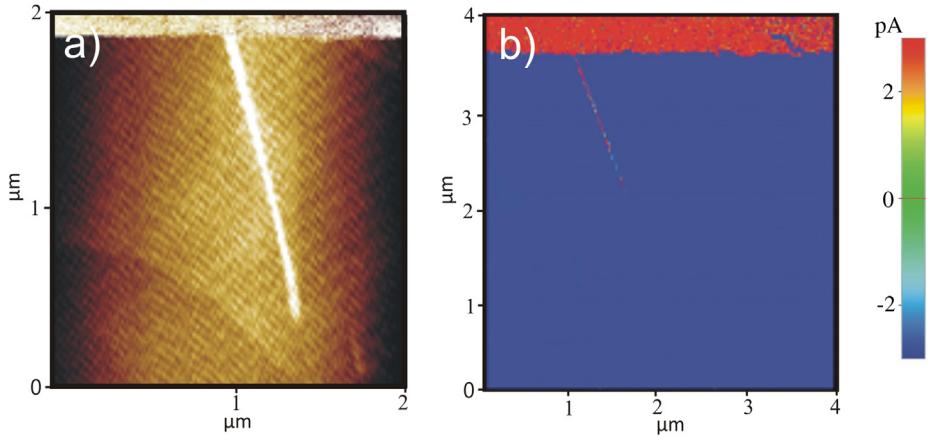

Fig. 7. (a) AFM topography image ($2 \times 2\ \mu m^2$) of single ZnChl-C6 nanowires spin-coated from THF/n-Hexane solution (1:99%) on a silicon oxide surface. Thickness of the gold layer ~40 nm; (b) Corresponding current image ($4 \times 4\ \mu m^2$) measured in the C-AFM mode. Tip bias: 1 V, sample bias: −1 V, set point: 153.68 (nN), scan rate: 0.63 Hz. (For interpretation of the references to color in this figure legend, the reader is referred to the web version of this article.)

Acknowledgments

This research has been financially supported by The Scientific and Technological Research Council of Turkey, TUBITAK (Grant: 110M803) and Polish National Science Center (844/N-ESF-EuroSolarFuels/10/2011/0) in the framework of European Science Foundation (ESF-EUROCORES-EuroSolarFuels-10-FP-006).

Appendix A. Supplementary data

Supplementary material related to this article can be found online at http://dx.doi.org/10.1016/j.nanoso.2017.02.002.

References

[1] F. Würthner, T.E. Kaiser, C.R. Saha-Möller, J. Angew. Chem. Int. Ed. 50 (2011) 3376–3410.
[2] S.S. Babu, D. Bonifazi, ChemPlus Chem. 79 (2014) 895–906.
[3] T.S. Balaban, H. Tamiaki, A.R. Holzwarth, Supermol. Dye Chem. 258 (2005) 1–38.
[4] M.R. Wasielewski, Acc. Chem. Res. 42 (2009) 1910–1921.
[5] G. De Luca, A. Romeo, V. Villari, N. Micali, I. Foltran, E. Foresti, I.G. Lesci, N. Roveri, T. Zuccheri, L.M. Scolaro, J. Am. Chem. Soc. 131 (2009) 6920–6921.
[6] M.A. Castriciano, A. Romeo, G. De Luca, V. Villari, L.M. Scolaro, N. Micali, J. Am. Chem. Soc. 133 (2010) 765–767.
[7] V. Huber, M. Katterle, M. Lysetska, F. Würthner, Angew. Chem. Int. Ed. 44 (2005) 3147–3151.
[8] S. Sengupta, D. Ebeling, S. Patwardhan, X. Zhang, H. von Berlepsch, C. Battcher, V. Stepanenko, S. Uemura, C. Hentschel, H. Fuchs, F.C. Grozema, L.D.A. Siebbeles, A.R. Holzwarth, L. Chi, F. Würthner, Angew. Chem. Int. Ed. 51 (2012) 6378–6382.
[9] C. Röger, Y. Miloslavina, D. Brunner, A.R. Holzwarth, F. Würthner, J. Am. Chem. Soc. 130 (2008) 5929–5939.
[10] T. Marangoni, D. Bonifazi, Nanoscale 5 (2013) 8837–8851.
[11] L. Maggini, D. Bonifazi, Chem. Soc. Rev. 41 (2012) 211–241.
[12] S. Ganapathy, G.T. Oostergetel, P.K. Wawrzyniak, M. Reus, A.G.M. Chew, F. Buda, E.J. Boekema, D.A. Bryant, A.R. Holzwarth, H.J.M. Groot, Proc. Natl. Acad. Sci. USA 106 (2009) 8525–8530.

[13] T.S. Balaban, Acc. Chem. Res. (38) (2005) 612–623.
[14] T.S. Balaban, M. Linke-Schaetzel, A.D. Bhise, N. Vanthuyne, C. Roussel, C.E. Anson, G. Buth, A. Eichhöfer, K. Foster, G. Garab, H. Gliemann, R. Goddard, T. Javorfi, A.K. Powell, H. Rösner, T. Schimmel, Chem. Eur. J. 11 (2005) 2267–2275.
[15] C. Chappaz-Gillot, P.L. Marek, B.J. Blaive, G. Canard, J. Bürck, G. Garab, H. Hahn, T. Jávorfi, L. Kelemen, R. Krupke, D. Mössinger, P. Ormos, C.M. Reddy, C. Roussel, G. Steinbach, M. Szabó, A.S. Ulrich, N. Vanthuyne, A. Vijayaraghavan, A. Zupcanova, T.S. Balaban, J. Am. Chem. Soc. 134 (2012) 944–954.
[16] G. Charalambidis, E. Kasotakis, T. Lazarides, A. Mitraki, A.G. Coutsolelos, Chem. Eur. J. 17 (2011) 7213–7219.
[17] W. Auwärter, D. Écija, F. Klappenberger, J.V. Barth, Nature Chem. 7 (2015) 105–120.
[18] S. Shoji, T. Ogawa, T. Hashishin, S. Ogasawara, H. Watanabe, H. Usami, H. Tamiaki, Nano Lett. 16 (2016) 3650–3654.
[19] T.S. Balaban, H. Tamiaki, A.R. Holzwarth, Top. Curr. Chem. 258 (2005) 1.
[20] S. Ganapathy, S. Sengupta, P.K. Wawrzyniak, V. Huber, F. Buda, U. Baumeister, F.rank Würthner, H.J.M. Groot, PNAS 106 (2009) 11472–11477.
[21] V. Huber, S. Sengupta, F. Würthner, Chem. Eur. J. 14 (2008) 7791–7807.
[22] V. Huber, M. Lysetska, F. Würthner, Small 3 (2007) 1007–1014.
[23] S. Shoji, T. Hashishin, H. Tamiaki, Chem. Eur. J. 18 (2012) 13331–13341.
[24] Y. Guo, L. Xu, H. Liu, Y. Li, C.M. Che, Y. Li, Adv. Mater. 27 (2014) 985–1013.
[25] X.F. Wanga, H. Tamiaki, Energy Environ. Sci. 3 (2010) 94–106.
[26] S. Erten-Ela, K. Ocakoglu, A. Tarnowska, O. Vakuliuk, D.T. Gryko, Dye. Pigment. (114) (2015) 129–137.
[27] S. Erten-Ela, O. Vakuliuk, A. Tarnowska, K. Ocakoglu, D.T. Gryko, Spectrochim. Acta Part A Mol. Biomol. Spectrosc. 135 (2015) 676–682.
[28] K. Ocakoglu, S. Erten-Ela, K.S. Joya, E. Harputlu, Inorg. Chim. Acta 439 (2015) 30–34.
[29] K. Ocakoglu, K.S. Joya, E. Harputlu, A. Tarnowska, D.T. Gryko, Nanoscale 6 (2014) 9625–9631.
[30] K.M. Smith, D.A. Goff, D.J. Simpson, J. Am. Chem. Soc. 107 (1985) 4946–4954.
[31] K.M. Smith, L.A. Kehres, J. Fajer, J. Am. Chem. Soc. 105 (1983) 1387–1389.
[32] H. Tamiaki, M. Amakawa, Y. Shimono, R. Tanikaga, A.R. Holzwarth, K. Schaffner, Photochem. Photobiol. 63 (1996) 92–99.
[33] M. Kasha, H.R. Rawls, M.A. El-Bayoumi, Pure Appl. Chem. 11 (1965) 371–392.